

## Gravity Probe B dewar/probe concept

R. T. Parmley, J. Goodman, M. Regelbrugge, S. Yuan

Research & Development Division, Lockheed Missiles & Space Company, Inc.  
Palo Alto, California 94304

### Abstract

Preliminary analyses and development tests are beginning to define the Gravity Probe B (GP-B) superfluid helium dewar and probe that contain the scientific instrument. The status of the current dewar and probe concept is reported, and supporting analyses used to define the neck tube region are described.

### Introduction

The GP-B is a new test of Einstein's General Theory of Relativity based on measuring with extreme precision in an Earth-orbiting satellite the precessions of gyroscopes with respect to a telescope pointed at a suitable guide star. The design of the experiment requires that the gyroscopes and reference telescope operate at liquid-helium (LHe) temperatures, and hence, that the entire mechanical portion of the scientific instrument be mounted in a long-hold-time liquid-helium dewar. This paper discusses the status of the analyses and design of the probe which holds the scientific instrument and the superfluid-helium (SFHe) dewar into which the probe is mounted.

### Preliminary design concept

Table 1 is a partial list of requirements that affect the probe and dewar design. Figure 1 presents the preliminary design status of the probe and dewar.

Table 1. Partial List of Requirements That Affect the Science Mission Probe/Dewar Design

1. Lifetime
  - 1 year minimum
  - 2 years desired
2. Probe inserted into cold dewar at a controlled rate
3. Reusable/refurbishable
4. Stiffness of QBA support/dewar  $\geq 20$  Hz
5. Spinup of gyroscopes
  - $f_{\text{spin}} \leq 170$  Hz
  - Helium spinup gas at gyro inlet
    - 5-8 K (+/- 0.25 K)
    - $\leq 60$  mg/s
    - $\leq 50$  torr
  - Helium spinup gas at gyro exhaust
    - $F_{\text{out}} \text{ (mg/s)} \leq 1.6 P_{\text{in}} \text{ (torr)}$
    - $P_{\text{out}} \leq P_{\text{in}}/10 \text{ (torr)}$
  - Helium leakage into probe near QBA
    - $\leq 0.14$  mg/s
    - $\leq 4.3 \times 10^{-4}$  torr
  - Sufficient boiloff for pointing plus roll rate of once per minute
6. Ultrahigh vacuum bakeout
  - QBA temp: + 2ΔK over operating
  - Ultimate pressure following bakeout  $\leq 10^{-10}$  torr
7. Science mission data taking
  - QBA temp: 1.5 to 2.5 K
  - $\leq 10^{-10}$  torr
  - $\leq 10^{-7}$  gauss
  - $\leq 10^{-10}$  g's
  - Sufficient boiloff for drag makeup, roll once per 10 minutes plus pointing (varies by a factor of 4 over lifetime)
  - Maximum allowable shift of satellite center of gravity
    - perpendicular to roll axis, 2 mm
    - parallel to roll axis, 110 mm
  - Slosh damping of SFHe

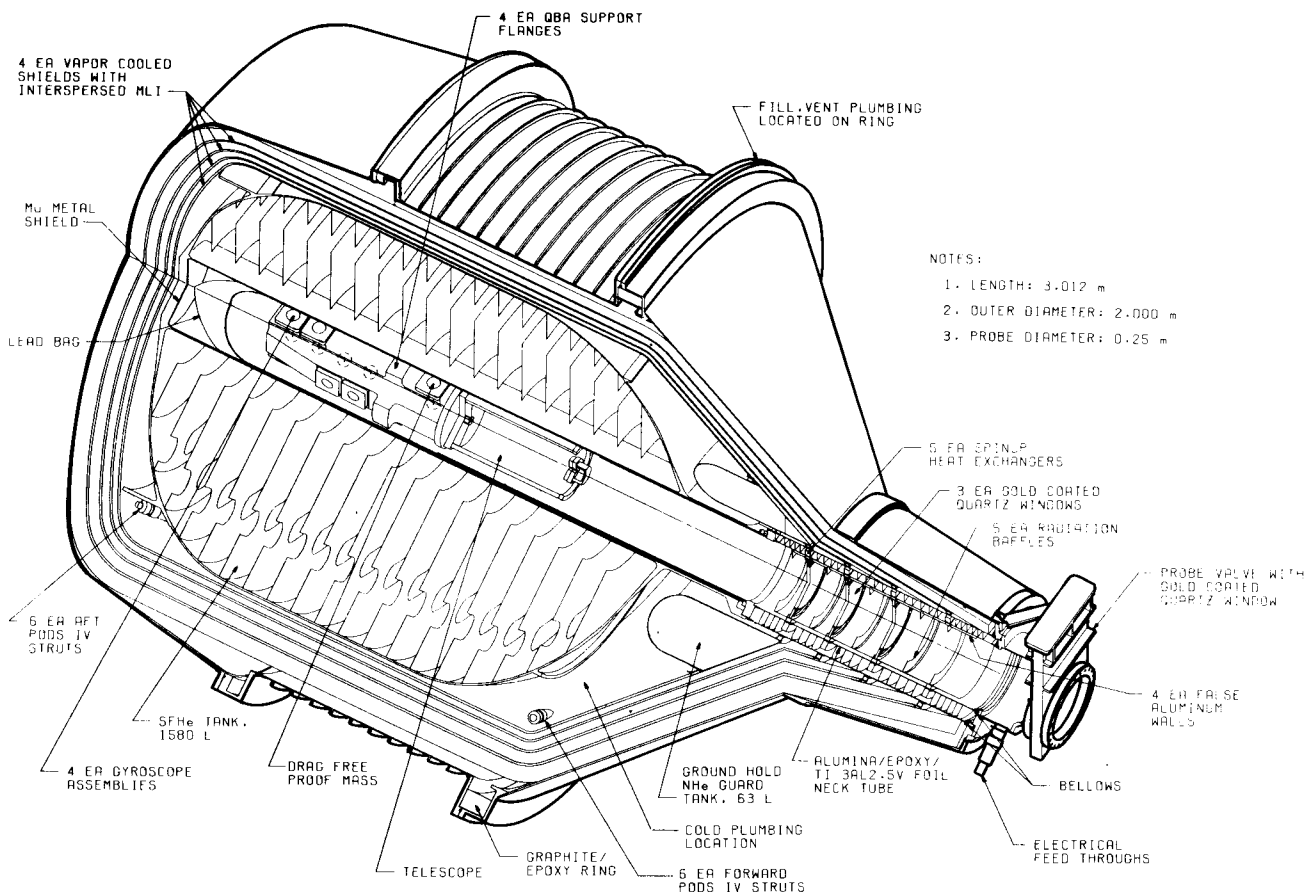


Figure 1. Preliminary probe/dewar concept.

## Probe

Major components of the probe are discussed first.

The scientific instrument consists of four gyroscopes, four SQUIDS and readout loops for measuring the gyroscope precession, six high-voltage electrodes for each gyroscope for suspending the gyroscopes, four gas inlet and four exhaust spinup plumbing lines (one set per gyroscope), and a drag-free proof mass used as a sensor in a control loop to keep orbital accelerations below  $10^{-10}$  g's. The four niobium-coated quartz gyroscopes and quartz drag-free proof mass are mounted in a quartz block assembly (QBA). A quartz telescope is mounted on the front end of the block. Four equally spaced quartz flanges on the QBA are bolted to an aluminum cylinder with five titanium bolts plus Belleville washers. The cylinder is slit into five fingers at each flange to minimize strain in the QBA during cooldown yet keep the QBA resonance  $\geq 20$  Hz. A removable probe vacuum shell provides service access to the instrument when the entire probe is removed from the dewar.

The aperture for the quartz telescope consists of an alumina/epoxy composite neck tube mounted off the end of the QBA aluminum support flange. A 0.5-mil 3.0Al 2.5V titanium foil is bonded on the inside surface to reduce the gas permeation and absorption rate.

Since the telescope views the earth over a portion of each orbit, three gold-coated quartz windows plus five gold-coated radiation baffles are used to reduce the radiation heat load. Gas leaking from the gyroscopes during spinup flows through the baffle aperture, around the window, and out through the probe gate valve to space. Following spinup and bakeout, the gate valve is closed because the required internal pressure is lower than space vacuum at 650 km. A gold-coated quartz window is mounted in the gate valve to allow viewing of the reference star Rigel.

Five counter-flow heat exchangers are used to cool the incoming warm helium gas during gyroscope spinup. The last heat exchanger uses a heater to control the spinup gas temperature to 5 to 8 K. A thermo-mechanical bolted joint grounds this heat exchanger to the dewar tank neck. Four thermo-mechanical disconnects with indium contacts are used to support and conductively ground the other four heat exchangers to the four vapor-cooled

shields in the dewar neck. The 3.0Al 2.5V titanium spinup plumbing lines are bonded to each heat exchanger on the outside diameter of the composite neck tube. All electrical feedthroughs penetrate the probe at the warm end of the neck. Electrical cabling is thermally grounded inside the neck aperture at each heat station. Four light pipe-readouts from the telescope are routed out in the same manner.

A cryopump is used to attain the  $<10^{-10}$ -torr pressure in conjunction with a low-temperature bakeout after gyro spinup.

#### Dewar

Major elements that make up the helium dewar are discussed here. A SFHe 1580-L toroidal, 6061-T6 aluminum tank provides the temperature environment, 2-year orbital lifetime, and mechanical support for the probe. An alumina/epoxy neck tube section extends from the tank neck to the vacuum shell and mates with the probe neck tube section. Both neck tubes terminate in welded bellows at the warm end. A 0.9-cm extension during tank cooldown would overstress the composite neck sections if they were not structurally decoupled from the vacuum shell. A compression stop on the bellows keeps the evacuated probe at the correct length during insertion into the dewar.

A 63-L normal-helium (NHe) guard tank is supported off the neck tube and grounded to the first of four vapor-cooled shields. The shield runs near 4.2 K on the ground with the SFHe tank near 1.7 K. The incoming heat boils off the helium in approximately 2 weeks. The NHe tank is vented continuously, while the SFHe tank is nonvented during the ground hold and launch phases of the mission. In orbit, after the remaining helium in the 63-L tank blows down, the SFHe tank is vented to space through a porous plug. This guard tank eliminates the need for continuous vacuum pumping on the SFHe tank during ground hold.

All loads to the vacuum shell from the two tanks, four vapor-cooled shields, multilayer insulation (MLI), and neck tube sections are taken out by 12 passive orbital disconnect struts (PODS-IV). (See Figure 2.) These struts, capable of both tension and compression loads, have a conductance approximately 10 times lower than nondisconnect fiberglass tension band straps both on the ground and in orbit. Under launch loads, the conductance is equal to or better than tension straps.

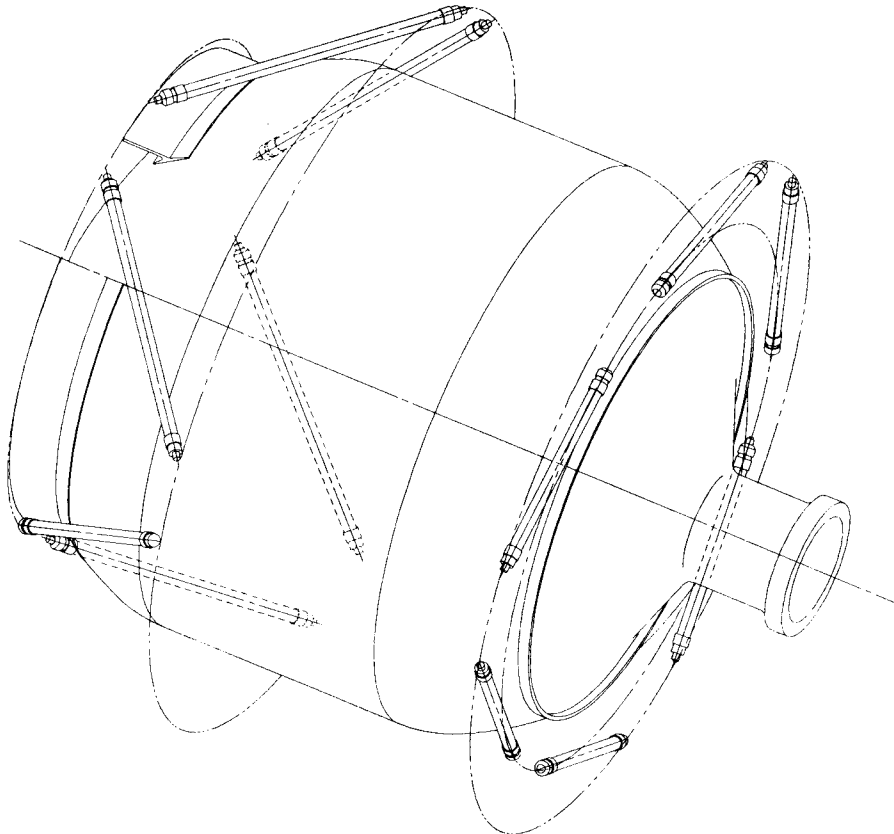


Figure 2. PODS-IV supports.

The six forward struts take out lateral, tilt, and torsional loads in conjunction with the six aft struts. All axial loads are removed through the six aft struts. This geometry prevents the PODS struts from shorting out due to thermally induced loads during tank cooldown. The six forward struts are mounted to a graphite/epoxy ring that changes little dimensionally with temperature. This composite ring prevents strut shorting due to thermally induced loads from vacuum shell temperature changes in orbit. These struts have been optimized to meet the launch loads, orbit resonance requirements, and thermally induced loads while minimizing the strut conductance.

Figure 3 shows the dewar plumbing schematic. All trapped volumes are protected by burst discs (tanks) or burst disc/relief valves (lines). Both tanks are filled through a single line: the SFHe tank through RAV-1 and the NHe tank through RAV-2. During cooldown and fill, the tank is vented through RAV3-4. A single vent line is also used for both tanks. When the NHe tank is empty in space, the SFHe tank is vented through porous plug PP2 and valve RAV-5 during gyroscope spinup operations when the heat rate is high (2.7 W). (See Figures 4 and 5.)

While science data are being taken, the tank is vented through porous plug PP1 when the heat rate is lower. However, there are times when atmospheric disturbances require that the vent rate to the control thrusters be increased by a factor of 4 to keep the proof mass from colliding with the cavity wall. Means to achieve this change in vent rate are under investigation. Five remotely actuated valves (RAV) are required to accomplish all these operations over a range of 1.5 to 40 K.

### Neck Tube Supporting Analyses

A number of supporting analyses and development tests are being performed to support the probe and dewar design effort. For the probe/dewar neck tube analyses, conflicting requirements (Table 2) require many design iterations before a reasonable compromise design can be achieved. Since all of the conflicts involve thermal performance, some simple thermal and gas flow pressure drop models were developed first. The scoping analyses based on these models showed that heat rate and pressure drop requirements during gyro spinup appeared to be achievable with a window/baffle arrangement similar to that shown in Figure 1.

This design was used as the starting point for detailed thermal analyses. The HEATRATERATE computer code was used to calculate view factors for various window and radiation baffle geometries. These view factors were then used with the THERM computer code model of the combined probe neck tube and dewar to calculate detailed temperature distributions and heat rates. Preliminary results indicate that windows and baffles spaced closer to the cold end of the probe (neck) minimize heat input (Figure 6).

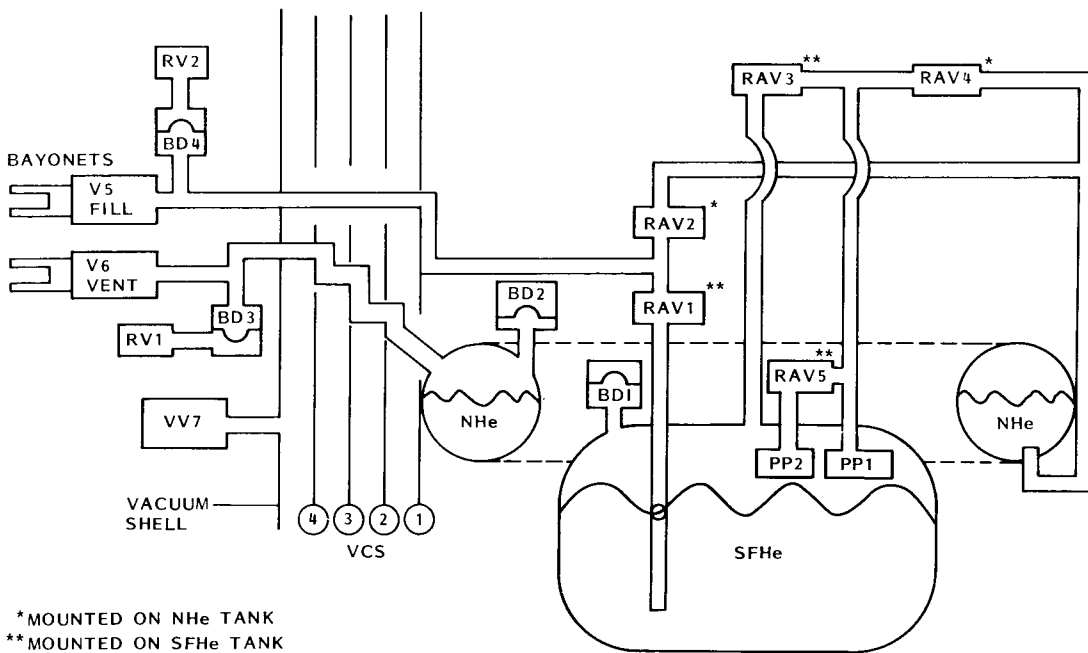


Figure 3. Preliminary dewar fluid schematic.

shields in the dewar neck. The 3.0Al 2.5V titanium spinup plumbing lines are bonded to each heat exchanger on the outside diameter of the composite neck tube. All electrical feedthroughs penetrate the probe at the warm end of the neck. Electrical cabling is thermally grounded inside the neck aperture at each heat station. Four light pipe-readouts from the telescope are routed out in the same manner.

A cryopump is used to attain the  $<10^{-10}$ -torr pressure in conjunction with a low-temperature bakeout after gyro spinup.

### Dewar

Major elements that make up the helium dewar are discussed here. A SFHe 1580-L toroidal, 6061-T6 aluminum tank provides the temperature environment, 2-year orbital lifetime, and mechanical support for the probe. An alumina/epoxy neck tube section extends from the tank neck to the vacuum shell and mates with the probe neck tube section. Both neck tubes terminate in welded bellows at the warm end. A 0.9-cm extension during tank cooldown would overstress the composite neck sections if they were not structurally decoupled from the vacuum shell. A compression stop on the bellows keeps the evacuated probe at the correct length during insertion into the dewar.

A 63-L normal-helium (NHe) guard tank is supported off the neck tube and grounded to the first of four vapor-cooled shields. The shield runs near 4.2 K on the ground with the SFHe tank near 1.7 K. The incoming heat boils off the helium in approximately 2 weeks. The NHe tank is vented continuously, while the SFHe tank is nonvented during the ground hold and launch phases of the mission. In orbit, after the remaining helium in the 63-L tank blows down, the SFHe tank is vented to space through a porous plug. This guard tank eliminates the need for continuous vacuum pumping on the SFHe tank during ground hold.

All loads to the vacuum shell from the two tanks, four vapor-cooled shields, multilayer insulation (MLI), and neck tube sections are taken out by 12 passive orbital disconnect struts (PODS-IV). (See Figure 2.) These struts, capable of both tension and compression loads, have a conductance approximately 10 times lower than nondisconnect fiberglass tension band straps both on the ground and in orbit. Under launch loads, the conductance is equal to or better than tension straps.

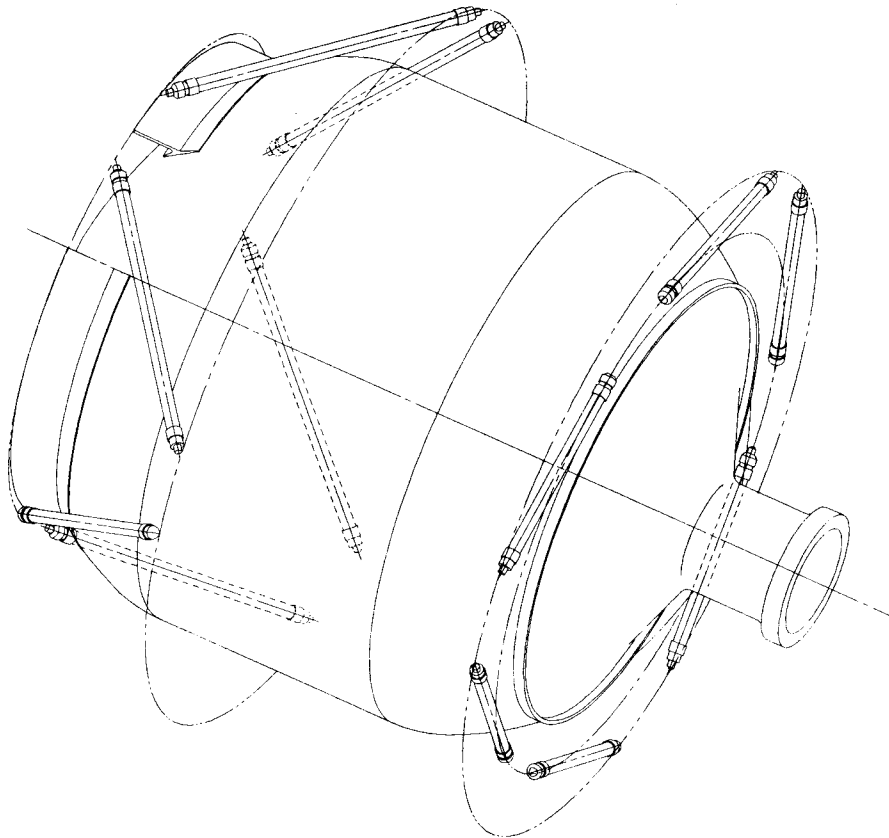


Figure 2. PODS-IV supports.

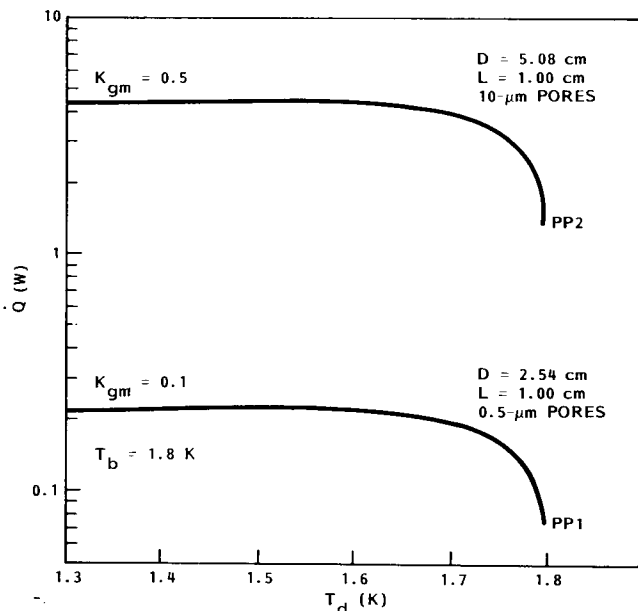


Figure 4. Porous plug downstream temperature versus heat rate.

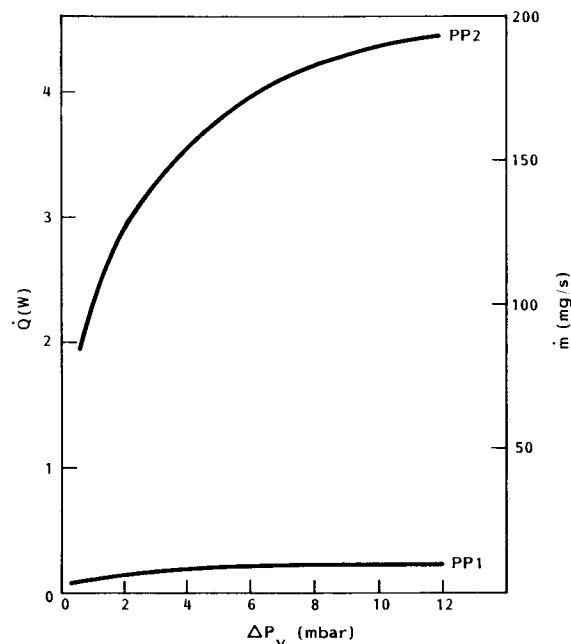


Figure 5. Porous plug pressure drop versus heat rate.

Table 2. Conflicting Neck Tube Requirements

<u>Thermal</u> Use gold-coated windows/baffles, minimize neck diameter	versus	<u>Gas Flow Conductance During Gyroscope Spinup</u> Increase diameter, remove as many windows and baffles as possible
<u>Thermal</u> Make neck tubes thin as possible	versus	<u>Structural</u> Design neck tubes for 1-atm loads (ground) and flight loads supporting NHe tank, vapor-cooled shields, and multilayer insulation
<u>Thermal</u> Solid connections between probe and dewar necks	versus	<u>Removable Probe</u> Joints with higher thermal resistance
<u>Thermal</u> Make neck tube as long as possible	versus	<u>Spacecraft Mass Balance</u> Make neck tube as short as possible
<u>Thermal</u> Use low-conductance materials	versus	<u>Gas Permeation</u> Use metal coating

This spacing also reduces the pressure drop through the neck tube and lowers the structural loads from the NHe tank. More analyses will be performed before window and baffle locations are set.

The detailed thermal model of the probe/dewar revealed a considerably different neck tube temperature distribution compared with the initial scoping analysis. Because of the low conductivity of the neck tube, the absorbed radiation causes temperature peaks between the window stations where the dewar vapor-cooled shields are connected (Figure 7). Since pressure drop is proportional to the square root of temperature in free molecular flow, and the flow regime in the neck tube is free molecular and transitional, the pressure drop calculated with these high wall temperatures is  $7 \times 10^{-4}$  torr, about 63% above the design goal of  $4.3 \times 10^{-4}$  torr near the gyros during spinup. This assumes that the leakage gas equilibrates with the temperature peaks along the neck tube wall. If the

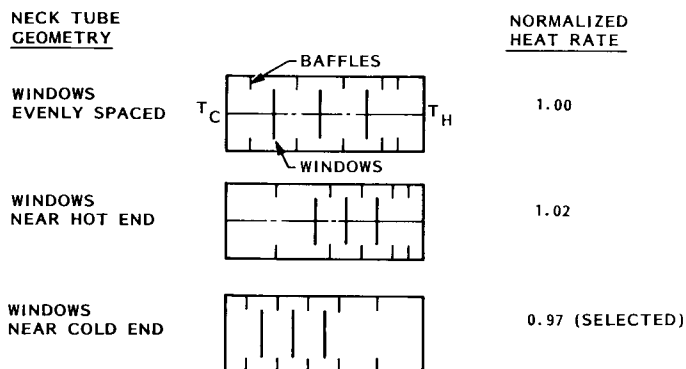


Figure 6. Total normalized heat rate into dewar for different window locations.

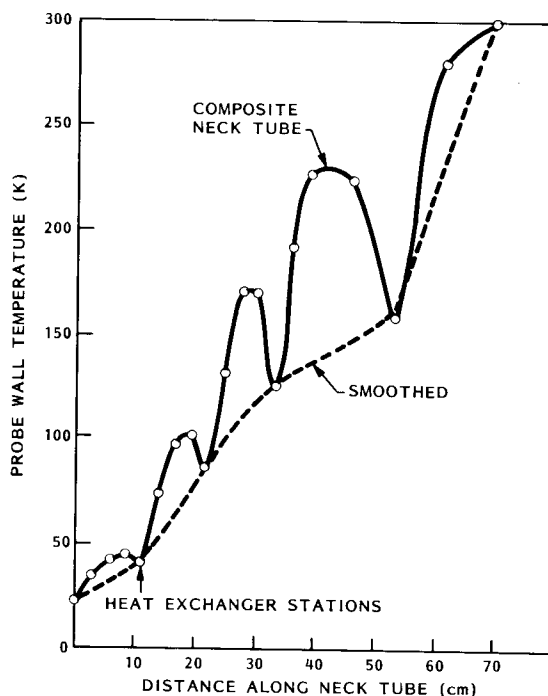


Figure 7. Probe neck tube temperature profiles.

pressure drop is calculated using gas temperatures in equilibrium with the smoothed temperatures between the vapor cooled shields, the pressure drop is  $6.4 \times 10^{-4}$  torr, still 50% above the design goal. Even with these lower temperatures and all windows and baffles removed, the calculated pressure drop is  $5.9 \times 10^{-4}$  torr, still 38% above the design goal. Further experimentally verified refinements to this model are needed before more accurate predictions of pressure drop can be made.

These calculations assume a 300-K vacuum shell for ground hold tests and shuttle orbital flight tests where lifetime requirements are 2 weeks or less. The neck tube temperatures for these tests can be depressed by increasing the boiloff rate with a heater and using "false" aluminum walls grounded to the heat exchangers to smooth out the temperature profile. For the 2-year science mission, the ambient temperature is near 220 K, helping to reduce the pressure drop and alleviate the gyro leakage venting problem. Other means that are currently being analyzed to reduce the pressure drop include increasing the neck tube diameter and using perforated baffles where the hole diameters are on the order of the infrared wavelength at a specified temperature. This baffle acts as a differential filter, passing helium gas yet appearing opaque to infrared radiation.

A  $\gamma$ -alumina/epoxy composite is being considered as a neck tube material, since its thermal conductivity is only slightly higher than E-glass/epoxy between 300 and 50 K and almost equal to graphite/epoxy below 50 K (Figure 8). Its Young's modulus is 10 percent lower than graphite and 2.3 times higher than glass. The axial conductivity of the composite was calculated versus wind angle (Figure 9), where 0 deg is parallel to the tube axis. The curves flatten at lower temperatures, where the conductivity of alumina and epoxy are almost equal. The 300-K curve was used in subsequent analyses.

Neck-tube optimization was analyzed using two versions of the PANDA program. The standard version determines, by iteration, a minimum weight design based on coalescence of buckling and strength failure modes at the applied loading. The other version determines a minimum conductance design subject to the same structural constraints by variation of thickness and winding angle parameters.

The former version was used to determine tube thicknesses for a 14.2-cm long tube with different ring spacings wound at 80 deg. Minimum ring cross-section dimensions were also determined for these cases, although the analyses showed very little sensitivity of the tube wall thickness to ring dimensions, and we felt that rings of the recommended dimensions were perhaps the lightest rings which could be reliably produced for this application.

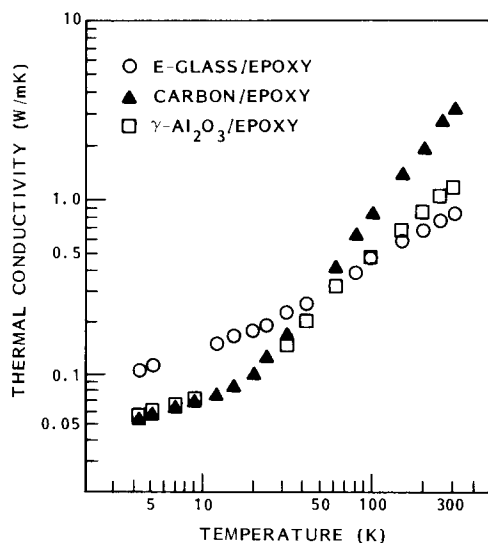


Figure 8. Thermal conductivity in the fiber direction.

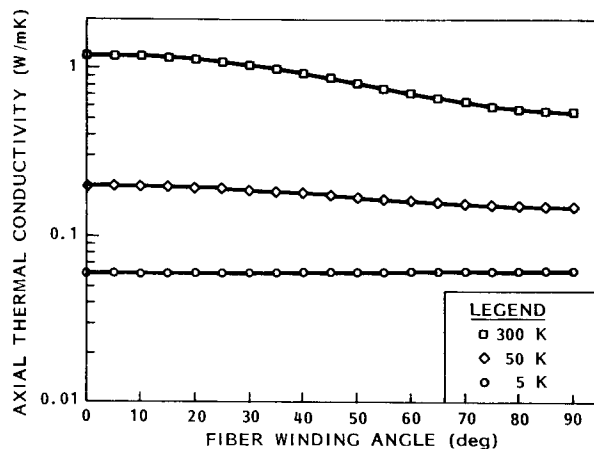


Figure 9. Thermal conductivity versus fiber angle for the alumina fiber composite.

The latter version was then used to determine the tube thickness and winding angle which produced minimum thermal conductance for each of the minimum weight designs. The figure of merit used to determine the final optimum design was the thermal conductance of the tube, including increased conductance due to the added ring material.

The loading used for the optimization analysis was 1 atm external pressure with a factor of safety of 2.0. The mechanical properties for the alumina/epoxy composite were assumed to be as listed in Table 3.

Table 3. Alumina/Epoxy Composite Mechanical Properties

Property	Value
Fiber-Direction Modulus ( $E_L$ )	86.9 GPa
Transverse Modulus ( $E_T$ )	2.76 GPa
Shear Modulus ( $G_{LT}$ )	1.03 GPa
Major Poisson's Ratio ( $\nu_{LT}$ )	0.25
Strain-to-Failure:	
Fiber Direction ( $\epsilon_{L_{ult}}$ )	0.40%
Transverse Direction ( $\epsilon_{T_{ult}}$ )	1.00%
Shear ( $\gamma_{LT_{ult}}$ )	1.00%

The results of the analyses are provided in Table 4. The optimum monocoque design is the first line in Table 4; the remaining cases are ring stiffened designs.

For the monocoque design, overall and local skin buckling modes are identical, and they occur at relatively low material strain levels. Hence, determination of a minimum thickness to satisfy buckling requirements is sufficient for structural design of monocoque neck tubes for pressure loading.

For ring stiffened designs, local skin buckling dominates the tube design to a ring spacing of 1.58 cm. At 1.42-cm spacing, the tube thickness required for stability becomes less than that required by the maximum strain capability of the material. Therefore, rings spaced closer than 1.58 cm will not provide any payoff with regard to thermal conductance, and the 1.6-cm ring spacing with a wall thickness of 0.05 cm (Table 4) is the optimum design for the probe.

Current analyses of the probe neck tubes are determining whether the optimum ring-stiffened design will also support flight loads imposed by the masses of the NHe tank, vapor-cooled shields, heat exchangers, MLI, and gold-coated quartz windows.

#### Acknowledgments

This work was performed under the Shuttle Test of Relativity Experiment (STORE) for the Leland Stanford Junior University as the prime contractor and NASA Marshall Space Flight Center.



Table 4. Optimum Designs for Ring-Stiffened Tubes  
With 1-atm Compressive Load

Ring Spacing (cm) (1)	Optimum Tube Wall Thickness (cm)	Optimum Winding Angle ( $\pm 0^\circ$ )	Effective Length (m)	Axial Thermal Conductivity (W/mK)	Conductance (3) ( $10^{-3}$ W/K)
14.22(2)	0.115	80.0	0.142	0.57	3.54
7.11	0.090	79.5	0.141	0.57	2.78
3.56	0.072	77.1	0.140	0.58	2.30
2.84	0.071	80.0	0.139	0.57	2.23
2.37	0.058	69.1	0.138	0.63	2.01
2.03	0.051	66.5	0.138	0.66	1.88
1.78	0.046	69.8	0.137	0.63	1.61
1.58	0.045	71.0	0.136	0.63	1.60
1.42	0.053	70.0	0.135	0.63	1.88

(1) Ring stiffeners are 0.76 mm thick by 3.2 mm high

(2) Tube held round at 14.2-cm intervals by heat exchangers

(3) Tube diameter = 24.4 cm

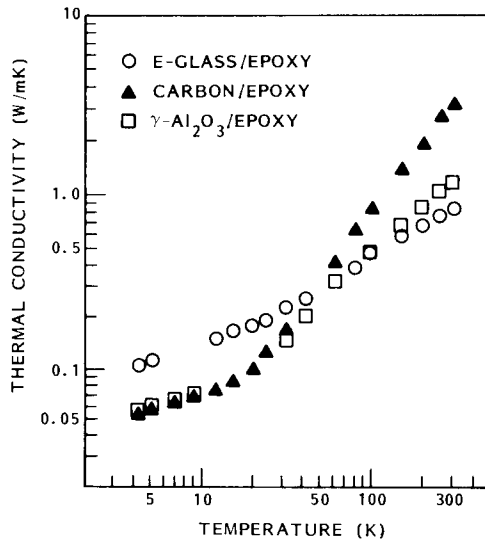


Figure 8. Thermal conductivity in the fiber direction.

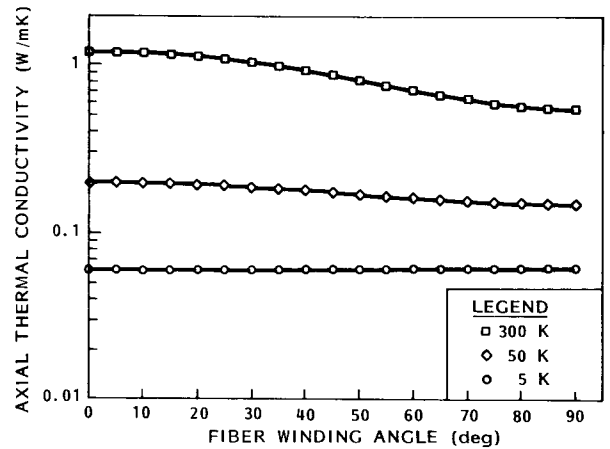


Figure 9. Thermal conductivity versus fiber angle for the alumina fiber composite.

The latter version was then used to determine the tube thickness and winding angle which produced minimum thermal conductance for each of the minimum weight designs. The figure of merit used to determine the final optimum design was the thermal conductance of the tube, including increased conductance due to the added ring material.

The loading used for the optimization analysis was 1 atm external pressure with a factor of safety of 2.0. The mechanical properties for the alumina/epoxy composite were assumed to be as listed in Table 3.

Table 3. Alumina/Epoxy Composite Mechanical Properties

Property	Value
Fiber-Direction Modulus ( $E_L$ )	86.9 GPa
Transverse Modulus ( $E_T$ )	2.76 GPa
Shear Modulus ( $G_{LT}$ )	1.03 GPa
Major Poisson's Ratio ( $\nu_{LT}$ )	0.25
Strain-to-Failure:	
Fiber Direction ( $\epsilon_{L_{ult}}$ )	0.40%
Transverse Direction ( $\epsilon_{T_{ult}}$ )	1.00%
Shear ( $\gamma_{LT_{ult}}$ )	1.00%

The results of the analyses are provided in Table 4. The optimum monocoque design is the first line in Table 4; the remaining cases are ring stiffened designs.

For the monocoque design, overall and local skin buckling modes are identical, and they occur at relatively low material strain levels. Hence, determination of a minimum thickness to satisfy buckling requirements is sufficient for structural design of monocoque neck tubes for pressure loading.

For ring stiffened designs, local skin buckling dominates the tube design to a ring spacing of 1.58 cm. At 1.42-cm spacing, the tube thickness required for stability becomes less than that required by the maximum strain capability of the material. Therefore, rings spaced closer than 1.58 cm will not provide any payoff with regard to thermal conductance, and the 1.6-cm ring spacing with a wall thickness of 0.05 cm (Table 4) is the optimum design for the probe.

Current analyses of the probe neck tubes are determining whether the optimum ring-stiffened design will also support flight loads imposed by the masses of the NHe tank, vapor-cooled shields, heat exchangers, MLI, and gold-coated quartz windows.

#### Acknowledgments

This work was performed under the Shuttle Test of Relativity Experiment (STORE) for the Leland Stanford Junior University as the prime contractor and NASA Marshall Space Flight Center.

Table 4. Optimum Designs for Ring-Stiffened Tubes  
With 1-atm Compressive Load

Ring Spacing (cm) (1)	Optimum Tube Wall Thickness (cm)	Optimum Winding Angle ( $\pm 0^\circ$ )	Effective Length (m)	Axial Thermal Conductivity (W/mK)	Conductance (3) ( $10^{-3}$ W/K)
14.22(2)	0.115	80.0	0.142	0.57	3.54
7.11	0.090	79.5	0.141	0.57	2.78
3.56	0.072	77.1	0.140	0.58	2.30
2.84	0.071	80.0	0.139	0.57	2.23
2.37	0.058	69.1	0.138	0.63	2.01
2.03	0.051	66.5	0.138	0.66	1.88
1.78	0.046	69.8	0.137	0.63	1.61
1.58	0.045	71.0	0.136	0.63	1.60
1.42	0.053	70.0	0.135	0.63	1.88

(1) Ring stiffeners are 0.76 mm thick by 3.2 mm high

(2) Tube held round at 14.2-cm intervals by heat exchangers

(3) Tube diameter = 24.4 cm